DOE Final Report May 2013

Title: Identification of genetic modifiers of susceptibility to radiation-induced lymphoma.

PI: Allan Balmain

Background.

The ultimate goal of this project is to identify the networks of genetic variants that confer susceptibility to the effects of low dose (0.1 Gy) γ-radiation, in particular with regard to tumor induction. In contrast to the known effects of high dose radiation in cancer induction, the responses to low dose radiation (defined as 0.1 Gy or less) are much less well understood, and have been proposed to involve a protective anti-tumor effect in some in vivo models. These conflicting results confound attempts to develop predictive models of the risk of exposure to low dose radiation, particularly when combined with the strong effects of inherited genetic variants on both radiation effects and cancer susceptibility. We are using a "Systems Genetics" approach that combines genetic background analysis with responses to low and high dose radiation, in order to develop insights that will allow us to reconcile these disparate observations. This comprehensive approach requires knowledge of the genetic architecture of normal tissue that is sensitive to development of radiation-induced tumors (in this case the skin and thymus), together with a view of the changes that take place in this architecture **a)** in response to low or high- dose radiation and **b)** during tumor development. It is also necessary to investigate the potential tumor-inducing or protective effects of low dose radiation in mice of the background used for these experiments (*129/Sv*).

Aim 1 applied a Systems Genetics approach to analyze the gene expression architecture of normal tissues from inter-specific mouse backcrosses as a basis for understanding the differential effects of exposure of these cells *in vivo* to low or high dose radiation. **Aim 2** identified p53 pathway-dependent mutations in radiation-induced lymphomas by whole genome sequencing and analysis of gene expression networks. Our revised **Aim 3** investigated the effects of the human Aurora-A kinase Phe31Ile polymorphism on radiation-induced lymphoma susceptibility using a unique knock-in mouse model.

Aim 1: Genetic architecture of normal mouse tissues and perturbation by low dose γ-radiation.

The development of cancer likely occurs along a continuum, with dynamic gene network changes in response to external stimuli/carcinogens. High doses of radiation (1-4Gy) are clearly carcinogenic, but the effects of low dose radiation (0.1 Gy or less) are controversial, as many studies suggest a protective rather than a causative role in radiation associated carcinogenesis. Our strategy proposed at the outset of this project was to **a)** analyze the genetic architecture of gene expression in normal tissues, and **b)** characterize the genetic pathways activated in tumors induced by γ-irradiation (0.1 Gy or 4Gy). This combined approach will identify the critical genes/pathways that have to be perturbed in order to develop tumors in radiosensitive tissues.

1a) Gene expression architecture in normal tail skin

The overall goal of Aim 1a) is to investigate the complex interactions that underlie the numerous functions of the p53 gene in vivo. Identification of p53 signaling networks in normal tissues may help to understand the genetic basis of susceptibility to different cancers, including lymphomas and skin cancers that involve perturbation of these pathways by either low or high dose of low LET γ-irradiation.

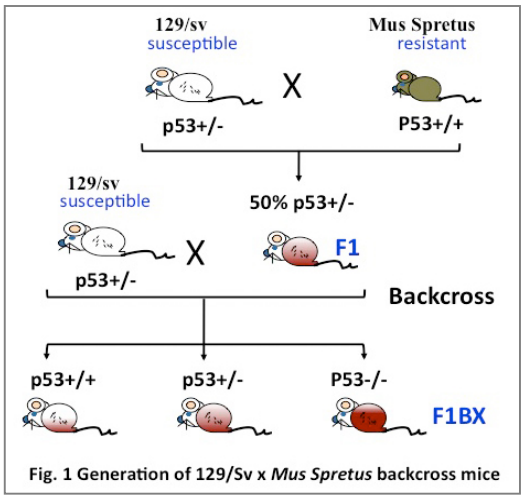

Fig. 1 Generation of 129/Sv x *Mus Spretus* backcross mice

During the first year of the DOE low dose grant appointment, we focused on breeding and harvesting tissues from inter-specific crosses between "radio-resistant and tumor-resistant" *Mus Spretus* and "radio-sensitive and tumor-susceptible" *129/Sv* on three different p53 genotypes (WT, HET, and KO for p53) as detailed in Fig. 1. This breeding scheme seeks to model complex heterogeneous human populations with varying tumor susceptibility. Sets of tissues (skin, tail, thymus, blood, spleen, kidney, lung, liver, pancreas, colon, and prostate/breast) were collected from 138 p53 WT (75 male, 63 female), 174 p53 HET (84 male, 90 female), and 66 p53 null (35 male, 31 female) F1Bx mice at the age of 8-weeks.

Figure 1. Generation of *129/Sv* x *Mus Spretus* backcross mice (*129BX*)
Spretus/Ei mice were crossed with *129/Sv* mice that are heterozygous null for p53 to generate F1 mice (50% $p53^{+/-}$, 50% $p53^{+/+}$). The $p53^{+/-}$ F1 mice were then backcrossed to the parental *129/Sv* ($p53^{+/-}$) mice to generate groups of F1 backcross (F1Bx) progeny with $p53^{+/+}$, $p53^{+/-}$ and $p53^{-/-}$ backgrounds. All F1Bx mice were sacrificed at the age of 8 weeks and various tissues including skin and thymus were collected for histology and extraction of RNA and DNA.

We initially profiled normal tail skin RNAs on Affymetrix Mouse Genome 1.1 ST gene expression arrays (89 WT, 62 HET, 62 KO, a total of 213 arrays) to construct genetic architectures of normal tail skin. Our strategy permits identification of the baseline genetic architecture of normal tissues, and may reveal the effect of p53 deletion on the rewiring of these gene networks. Furthermore, these data will provide a basis for comparison with parallel data from irradiated skin or tumor samples.

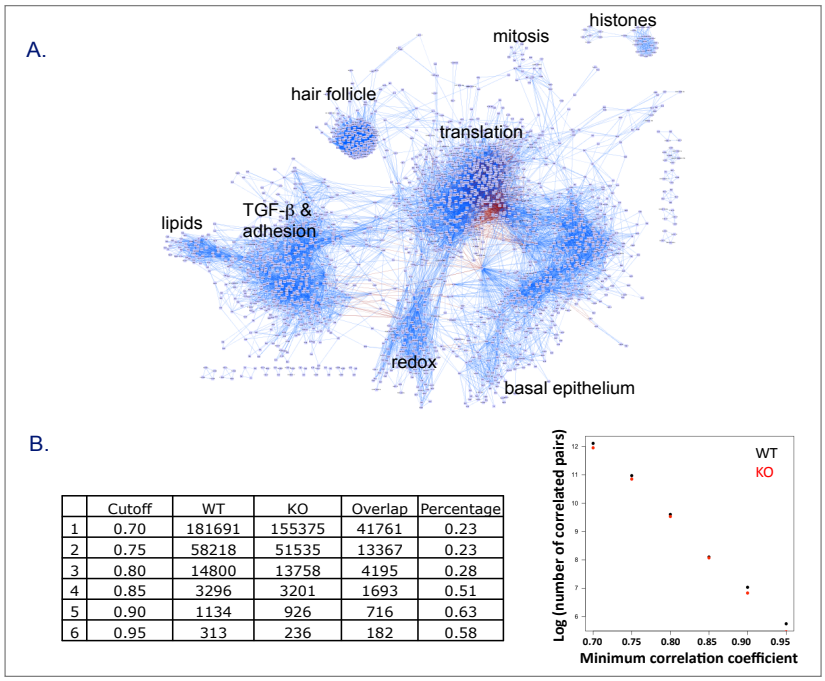

	Cutoff	WT	KO	Overlap	Percentage
1	0.70	181691	155375	41761	0.23
2	0.75	58218	51535	13367	0.23
3	0.80	14800	13758	4195	0.28
4	0.85	3296	3201	1693	0.51
5	0.90	1134	926	716	0.63
6	0.95	313	236	182	0.58

A network view of the gene expression architecture of 129BX tail skin from both WT and KO mice is shown in Fig. 2A. The table and plot in Fig. 2B summarize the numbers of correlated gene pairs at different minimum correlation coefficients. While similar numbers of correlation events are present between WT and KO, the overlap between the two genotypes at <0.8 was less than 28%. This suggests that the tail skin genetic architecture is rewired by the deletion of p53.

Figure 2. A visual representation of the *129BX* tail skin gene expression network
A) Gene expression correlation networks were derived from the 89 WT and 61 p53 KO tail skin. Network edges connect significantly correlated genes (blue squares) that are co-regulated in cliques with five or more members. R^2 cutoff of 0.85 was used. Labels identify clusters significantly enriched for functional or structural properties. **B)** A table and a plot describing numbers of correlated gene pairs at different minimum correlation coefficients.

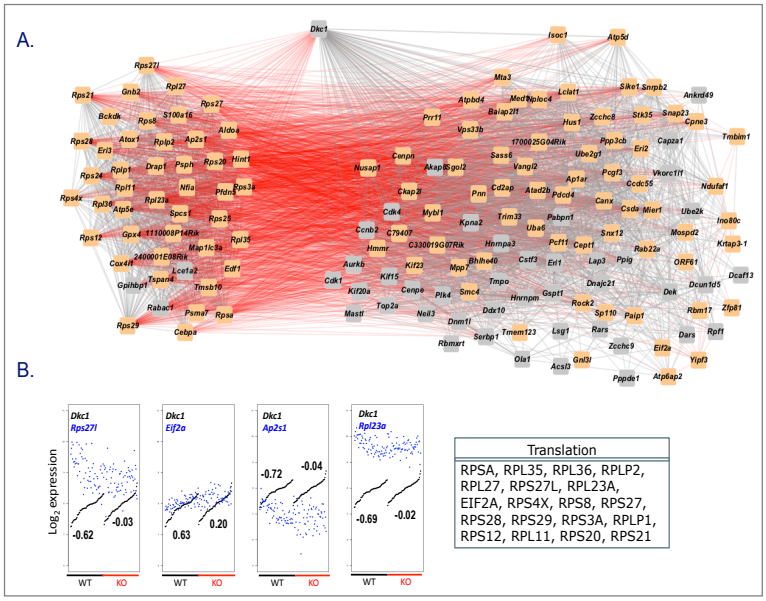

Gene expression differential correlation analysis showed that *Dkc1*, a pseudouridine synthase, is tightly correlated with multiple genes involved in translation and mitosis in tail skin from WT mice (Fig. 3). In this network, red edges represent negative gene expression relationships between the genes, while the gray edges represent positive relationships. Interestingly, the majority of these correlations between Dkc1 and ribosome biogenesis factors (genes in light yellow) are lost in tail skin from p53 KO mice, suggesting that the Dkc1 network is significantly rewired in the absence of p53.

Figure 3. Rewiring of the Dkc1 network in p53 KO tail skin
A) *Dkc1* is negatively correlated with many ribosomal protein genes (*Rps* and *Rpl* genes), while it is positively correlated with mitotic cell cycle and other RNA processing genes in the WT tail skin. Interestingly, many of these genes (yellow squares) lose the tight correlations in the KO tail skin. **B)** Example plots demonstrating high correlation between *Dkc1* and *Rpl27l, Eif2a, Ap2s1, and Rpl23a* in the WT but not in the KO tail skin. Many of the differentially correlated genes are involved in translation categorized by DAVID Gene Ontology analysis.

Our data suggest that several gene networks that are involved in metabolic processes, immune responses, and multiple RNA processing pathways such as RNA splicing and translational control are rewired in the absence of p53. Future work will focus on elucidating how p53 regulates Dkc1 functions using functional biochemical assays and *in vivo* mouse work.

1b) Assessment of the effect of Low Dose γ-irradiation on tumorigenesis risk

The original Aim 1b) is to examine the effects of low dose γ-radiation on the genetic architecture of normal thymus from the inter-specific backcross mice generated in 1a). Prior to generating an irradiated backcross population, we conducted an initial study investigating the long-term impact of low dose γ-radiation upon tumor formation using tumor susceptible *129/Sv* parental mice. The test group *129/Sv* $p53^{+/-}$ mice (n=32, 16 female, 16 male) received 0.1 Gy of whole body γ-radiation (dose rate – 0.233Gy/min) and the control group mice were un-exposed (n=21, 11 female, 10 female). All mice were checked at least three times weekly for tumor formation and toxicity from the treatment. Normal and abnormal tissue including tumors, from thymus, spleen, skin and tail were harvested.

We finished this study on 3/12/2013, as all mice reached our set end point (survival time ≥ 600 days). The survival curves of the two groups were not significantly different as shown in Fig. 4A (Log-rank (Mantel-Cox) test, P=0.48), and the median survival was also similar between the two groups (0.1Gy-546 days, Con-559 days). This suggested that 0.1Gy of low dose radiation exposure did not have a protective nor hazardous effect on overall mouse survival. H&E slides were prepared from the tumor samples and examined by Dr. Kuang-Yu Jen, a pathologist, to determine the histologic subtypes of the tumors. Interestingly, the $p53^{+/-}$ mice irradiated with 0.1 Gy γ-radiation developed a range of different types of tumors compared to the control group mice (Fig, 4B). Although this could potentially suggest that low dose γ-radiation might shift the tumor spectrum of these mice, we cannot exclude the possibility that this is simply due to the

relatively small, and unequal sample size between the Con (n=21) and the irradiated (n=32) group. We are currently analyzing the subtypes of these tumors by immunohistochemistry/flourescence and microscopy analysis for various tumor markers such as Vimentin, CD31, CD34, and Keratins.

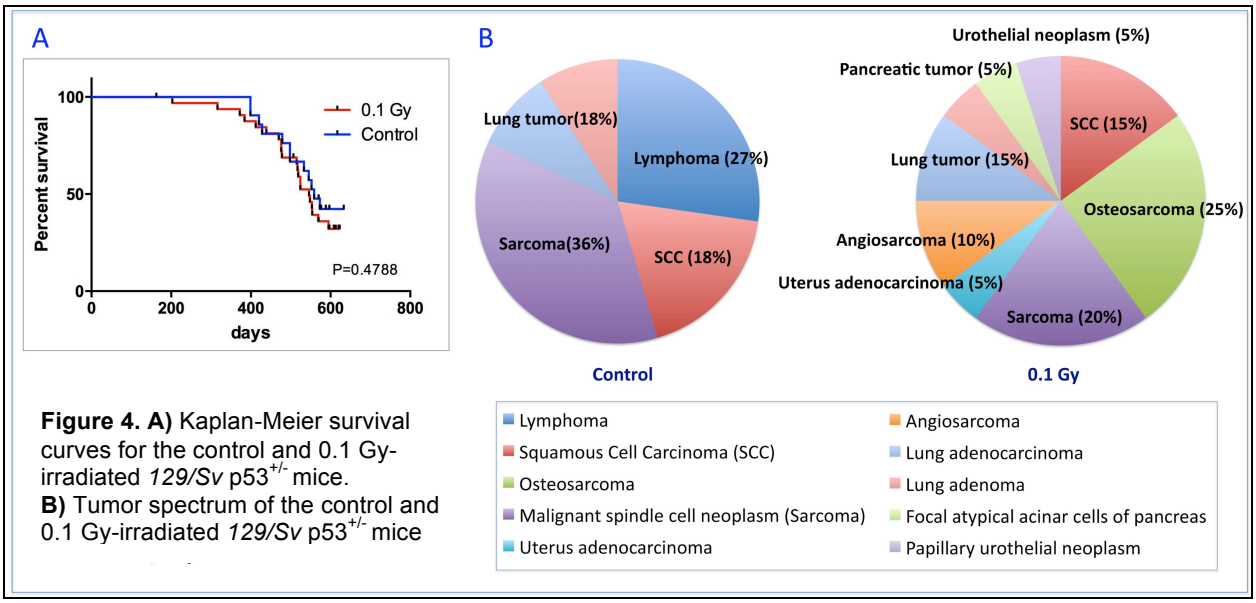

Figure 4. A) Kaplan-Meier survival curves for the control and 0.1 Gy-irradiated *129/Sv* $p53^{+/-}$ mice.
B) Tumor spectrum of the control and 0.1 Gy-irradiated *129/Sv* $p53^{+/-}$ mice

1c) Measurement of dynamic changes in gene expression as a function of radiation dose and time after exposure

The focus of Aim 1c) is to analyze the dynamic changes, which occur over time after radiation exposure in the normal tissues. The development of cancer likely occurs along a continuum, with dynamic gene network changes in response to external stimuli/carcinogens. To study temporal changes in radiation response, we irradiated 8 week-old mice of three different p53 genotypes (*129/Sv* strain) using either 0.1Gy or 4Gy (4 mice of each genotype for each radiation dose and time point). Cs^{137} was the source of γ-radiation, and the dose rate delivered was 0.233Gy/min. Radiosensitive tissues including the thymus, blood and spleen, as well as less sensitive tissues including skin, liver, and lung were harvested at 4, 24 hours, 1 week, and 1 month post-radiation exposure as shown in table 1. RNAs from skin (4hr, and 1 month, a total of 72 arrays) and thymus tissues (4, 24hr, and 1 month, a total of 96 arrays) were profiled on Affymetrix Mouse Genome 1.1 ST gene expression arrays. This approach allows for detection of fluctuations in the normal gene network in response to subtle interrogation of the network with low or high dose radiation. This approach will identify early vs. late response gene networks and monitor their activity over time. It will also distinguish gene networks responding to low or high dose radiation, and also those responding to both insults. Moreover, genes that are differentially regulated with regard to p53 status will be identified.

Table 1. Time-course to evaluate the effects of low and high dose γ-radiation on mouse tissues

Genotype	Sham	0.1Gy	4Gy	0.1Gy	4Gy	0.1Gy	4Gy	Sham	0.1Gy	4Gy	TOTAL
129/Sv	4hrs			24hrs		1 week		1 month			
p53 +/+	4	4	4	4	4	4	4	4	4	4	40
p53 +/-	4	4	4	4	4	4	4	4	4	4	40
p53 -/-	4	4	4	4	4	4	4	4	4	4	40

Our data analysis from the skin gene expression arrays of 4hr and 1-month timepoints suggested that minimal, if any, statistically significant differences in gene expression were detectable in skin at 4 hours after exposure to low dose (10cGy) radiation (Genes are at 10% FDR and have fold-change <0.75 or >1.25). In contrast, high dose exposure elicited changes in some of the known mitotic cell-cycle genes including Aurora-A kinase, Cenpe, and cyclin B1. On the other hand, some statistically significant changes in gene expression were detected in the skin at one month after low dose exposure including those involved in RNA processing, cell adhesion, and muscle contractility (Table 2). Although many of the changes seen are in biologically relevant pathways, it will be necessary to exclude technical artifacts including the age of the mice and contamination with muscle components before reaching any definitive conclusions regarding induction by low dose radiation.

Table 2. Differentially expressed genes/pathway by low or high dose γ-radiation in mouse tail skin

	4 hr		1 month	
	0.1 Gy	**4 Gy**	**0.1 Gy**	**4 Gy**
WT	None	Ctgf, Polk, Icam1, Bcl3, apaf1	Muscle System	Muscle System
HET	Intracellular Signaling Cascade	Hair cycle, epidermis development	Transcription, RNA processing	Mtap1s, Krt16, Lce1i
KO	Ctgf, Ddit4, Pde1a	Mitotic Cell Cycle	Cell adhesion	Immune Responses

In addition, we analyzed gene expression patterns of the more radiosensitive thymus tissues from the same animals (4, 24hr, and 1 month, a total of 96 arrays). Similar to the tail skin, no genes were differentially expressed at 4 hours after exposure to low dose with our statistical cutoff of genes at FDR<10% with fold-change <0.75 or >1.25, SAM. On the other hand, high dose radiation altered gene expression patterns of more than 450 genes in the WT thymus at 4 hours after exposure to 4 Gy of radiation (Fig. 5). Most of these genes are in the canonical radiation response pathways such as apoptosis, DNA repair/replication, and immune responses. Interestingly, these genes were not significantly different in the tail skin of these animals at 4hr, demonstrating tissue-specificity in radiation responses.

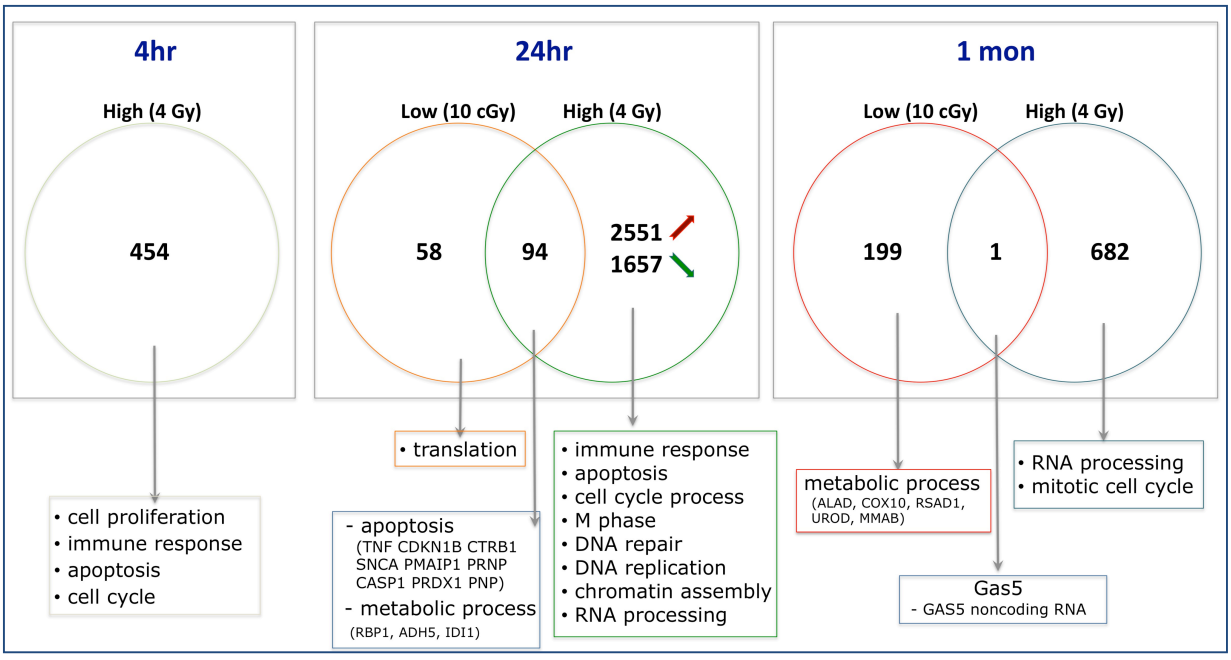

Figure 5. Venn diagrams illustrating gene overlap across radiation doses in the mouse thymus
Left Panel: No genes were differentially expressed by 0.1Gy of γ-radiation after 4 hr of exposure. In contrast, 4Gy induced gene expression changes in cell proliferation, immune response, apoptosis, and many phases of cell cycle at 4 hr. **Middle Panel**: Genes involved in translation were altered by low dose radiation at 24 hr, while more canonical radiation response genes/pathways were regulated by high dose radiation. **Right Panel**: RNA processing genes were persistently induced by high dose radiation at 1 month post-treatment. Few genes overlapped between 0.1Gy and 4Gy for all three time-points evaluated, suggesting that radiation responses to low and high dose radiation exposure are qualitatively different.

At 24 hrs, 150 genes were differentially expressed by 0.1Gy while more than 4000 genes were changed by 4Gy, suggesting that radiation responses to low and high doses differed "quantitatively". While 94 genes functioning in apoptosis and metabolic processes were differentially expressed by both low and high doses, 58 genes were induced specifically only by 0.1Gy, but not by 4Gy. This suggested "qualitatively" different responses between low and high doses. This pattern was more evident at 1 month after exposure, as only 1 gene (Gas5) was in the intersection between 0.1Gy and 4Gy responsive genes. Therefore, our data demonstrates non-linear response with respect to doses, and does not support the Linear-No Threshold (LNT) model.

Gene expression modulation was more transient by low dose, as only 2 genes overlapped between 24hr and 1 month post-exposure by 0.1Gy (Fig. 6). On the other hand, a more persistent pattern was observed for high dose. 283 genes were in the intersection between 24hr and 1 month after 4Gy exposure, and these genes function in mitotic cell cycle, DNA repair/replication, as well as RNA processing.

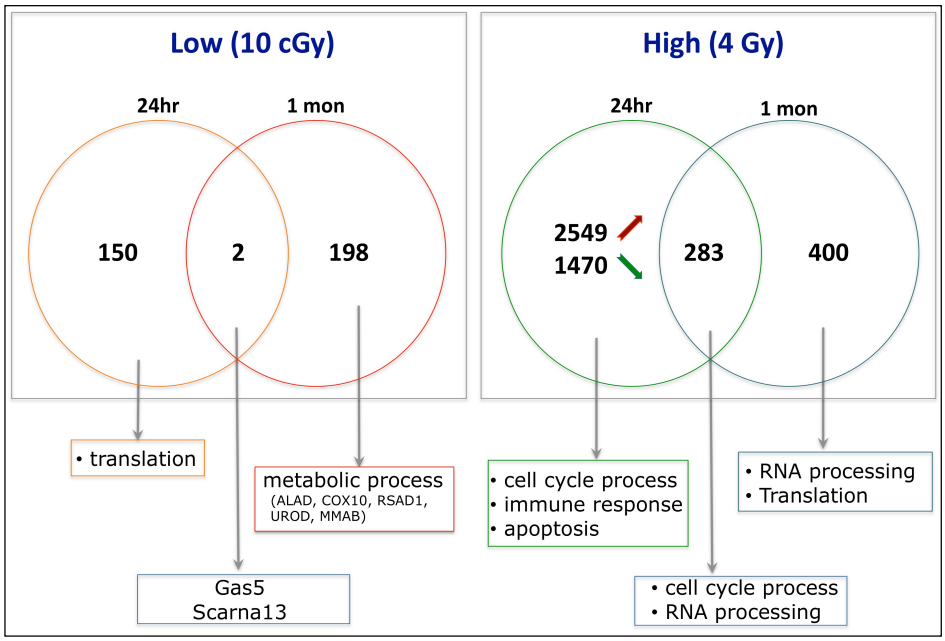

Figure 6. Venn diagrams illustrating gene overlap across post-irradiation times in the mouse thymus.
Left Panel: Comparison between significantly differentially expressed genes at 24 hr and at 1 month in response to 0.1Gy. **Right Panel**: Comparison between significantly differentially expressed genes at 24 hr and at 1 month in response to 4Gy.

We are also investigating genes that are differentially regulated with regard to p53 status. The analysis is currently incomplete, but our preliminary data suggests that response patterns of many cell cycle and inflammatory genes including Bax, Aurkb, and Ccl7 are altered by p53

status. Interestingly, we also found that RNA processing genes in the Dkc1 network including Dkc1, Nolc1, Nop2, Nhp2, Gnl3 and Naf1 are differentially expressed in a p53-dependent manner after radiation exposures. Future work will further focus on elucidating crosstalk between p53 and Dkc1 networks.

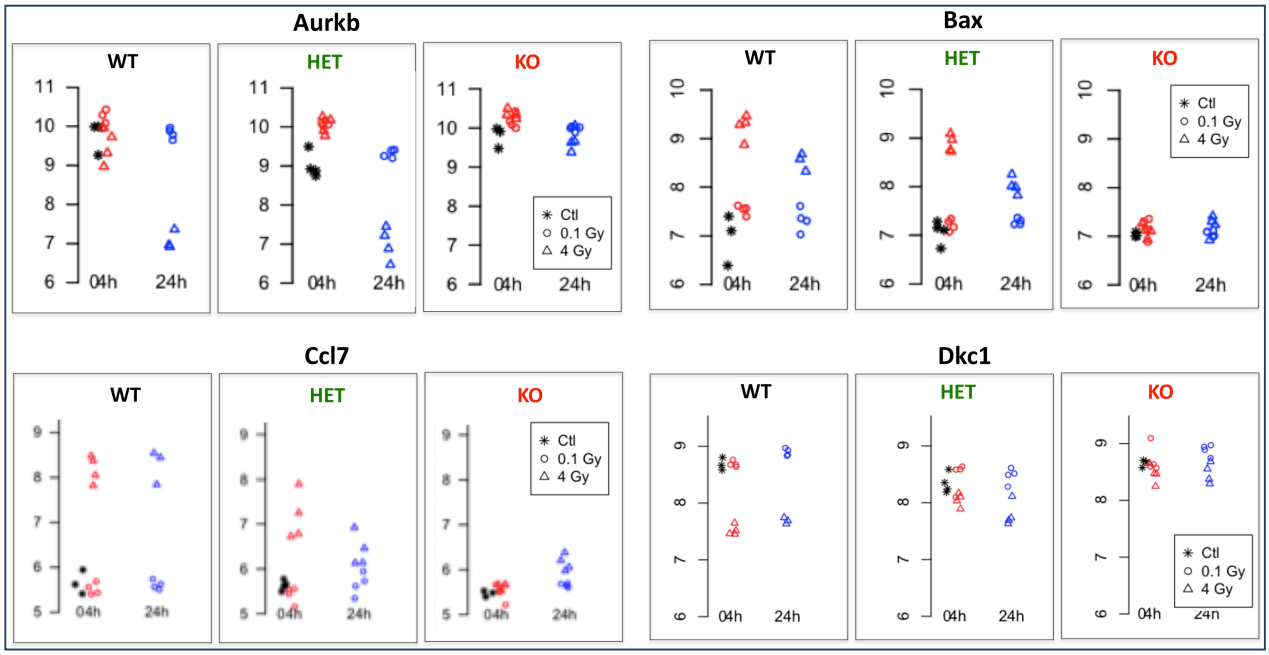

Figure 7. Expression plots showing p53-dependent radiation responses
Gene expression levels of Aurkb, Bax, Ccl7, and Dkc1 in the thymus from mice irradiated with 4Gy of γ-radiation at 0, 4hr, and 24hr post-radiation are shown. These plots demonstrate that radiation responses of Aurkb, Bax, Ccl7, and Dkc1 to high dose (4Gy) radiation are p53-dependent.

Aim 2: Genetic architecture of gene expression in relation to radiation-induced lymphoma development.

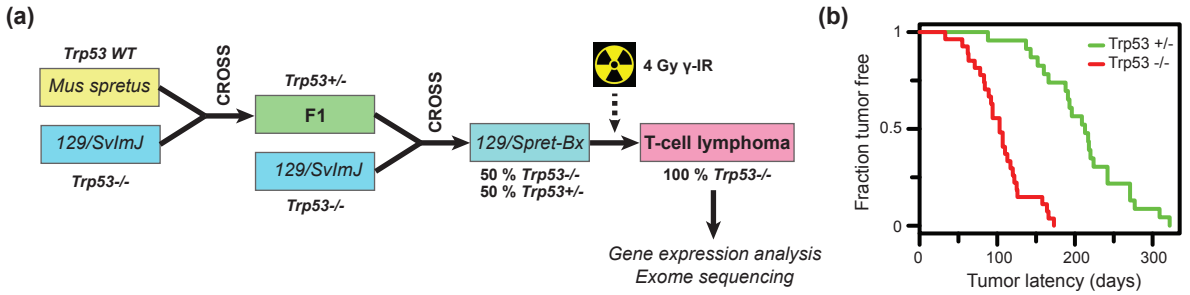

Figure 8. Outline of Aim 2. (a) Mouse cross, genotypes and workflow. (b) Tumor latency as a function of Trp53 germline genotype ($p<0.001$; log-rank test).

Previous genetic analyses have shown that irradiation-induced lymphomas from *Trp53* heterozygous mice undergo genomic changes that are not detected in tumors from *Trp53* null mice[1]. While both tumor classes show activating mutations to Notch1, tumors from *Trp53*+/- mice also show preferential loss of the *Fbxw7* tumor suppressor and 100 % loss of the remaining functional *Trp53* allele. These results indicate that although the two classes of tumors

are in fact null for *Trp53*, they undergo distinct sets of genetic changes during tumor progression. We extended these previous results by employing next-generation exome sequencing in combination with gene expression network analysis of irradiation-induced T-cell lymphomas from a 129/SvImJ x spretus interspecific backcross population (Fig. 8a-b). Interestingly, only about 100 genes were significantly differentially expressed between the two tumor classes (rank-product test), however gene expression network analysis identified a network with modules that could be functionally annotated to e.g. Notch-signaling, T-cell receptor signaling and tumor cell differentiation stage (Fig. 9a).

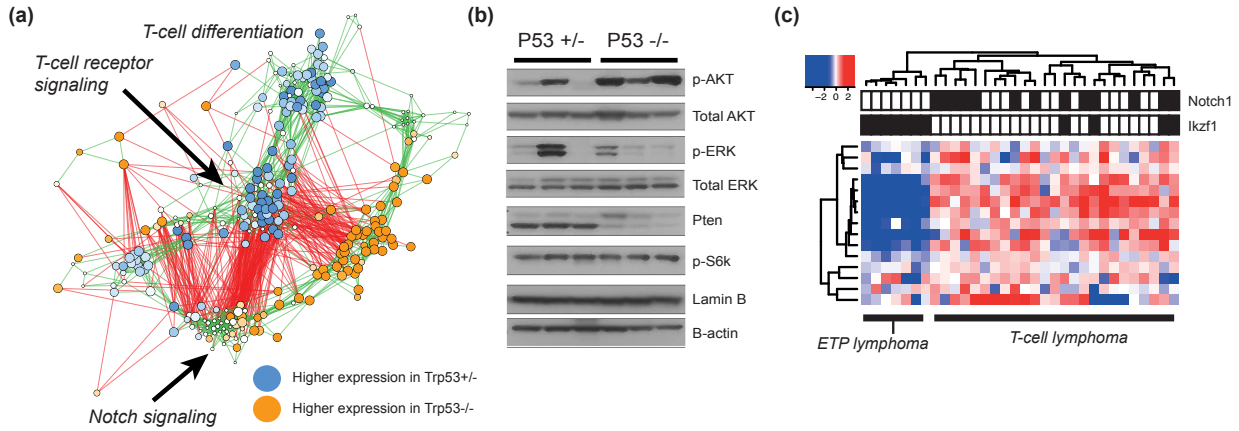

Figure 9. Integrated analysis of gene expression and exome sequencing data identify tumor subtypes and signaling pathway activation in irradiation-induced T-cell lymphomas. (a) Gene expression network analysis was performed by connecting genes (nodes) by edges for pair-wise absolute Spearman correlations larger than 0.7. Green and red edges represent positive and negative correlations, respectively. Differentially expressed genes are visualized as blue and orange nodes. (b) Western blot analysis of PI3K and MAPK pathway proteins. (c) Hierarchical clustering associates Ikzf1 loss with a gene expression signature representing Early T-cell Precursor leukemia.

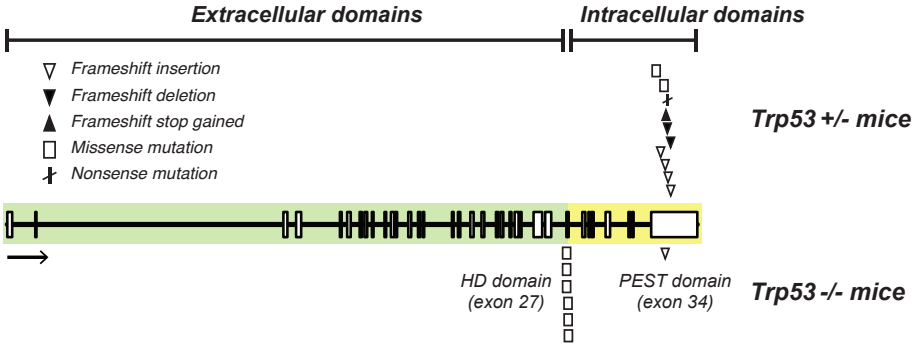

Figure 10. Distribution of *Notch1* mutations identified by exome sequencing of 32 T-cell lymphomas.

Activating mutations to *Notch1* is a hallmark for human T-ALL development and mutations generally target the HD or PEST domains. HD domain mutations are considered a more potent oncogenic activation of Notch-signaling whereas PEST domain mutations require additional activation of oncogenic pathways such as Ras[2]. Interestingly, we find HD domain point mutations exclusively in tumors from *Trp53*-/- mice, whereas tumors from *Trp53*+/- mice had PEST domain point or indel mutations (Fig. 10). Of note, while more than 40 % of T-ALL patients carry HD domain mutations [3], they have very rarely been described in mouse models [4]. Strikingly, several of the *Notch1* mutations were exactly synonymous to human cancer and we also identified synonymous mutations to *Idh1* (R132 hotspot) and *Trp53* (R175H hotspot), thus

emphasizing the clinical relevance of our model. Further comparison of mutational spectra between tumors emanating from the two different *Trp53* genotypes showed preferential copy-number or mutational loss of the tumor suppressors *Pten* and *Inpp4b* [5] in tumors from *Trp53*-/- animals suggesting p53-related activation of the PI3K pathway. This was supported by Western blot analysis of key proteins in the MAPK and PI3K pathways (Fig. 9b) suggesting that tumors activate different signaling pathways depending on germline genotype. The T-cell receptor (TCR) module was more highly expressed in *Trp53*+/- derived tumors and contained several genes related to activation of the Ras/MAPK pathway (*Egr1*, *Rasgrp1*, *Dusp4*). However, Western blot analysis of MAPK pathway proteins did not give conclusive results (Fig. 9b).

Mutation expression Quantitative Trait Loci (eQTL) analysis identified a significant connection between loss of *Ikzf1* (point mutation or deletion) and low expression of the Notch1-related gene expression module ($p<0.001$) (Fig. 9a). A recent publication implicated *IKZF1*-loss in Early T-cell Precursor (ETP) leukemia, a highly aggressive leukemia subtype[6]. Our *Notch1* gene expression module (Fig. 9a) overlapped with a published ETP leukemia gene expression signature[6] and based on this gene expression pattern in conjunction with *Ikzf1* loss, we identified several of our lymphomas as ETP (Fig. 9c). Importantly, in our mouse lymphoma data the ETP signature genes are not differentially expressed between *Trp53*+/- and *Trp53*-/- derived tumors (Fig. 9a). Thus the ETP samples could not have been identified with conventional gene expression analysis assaying differential expression between a priori known sample classes. In conclusion, our analyses show that the p53 irradiation-induced lymphoma model is highly relevant for human T-ALL. Interestingly, in our previous analyses of *Notch1* mutations in thymic lymphomas from pure-bred 129/Sv mice we have only found PEST-domain mutations irrespective of p53 germline genotype[7]. Thus the *Spretus* backcross introduces tumor resistance loci that act as modifiers of tumor development leading to a mutational spectrum more similar to human cancer. Future studies will focus on detailing the sequence of mutational events in lymphomas from *Trp53* heterozygous and null mice respectively. Furthermore, we investigate the usefulness of this model in development of targeted treatment.

Aim 3. The human Aurora-A kinase Phe31Ile polymorphism affects cancer susceptibility in a knock-in mouse model

Our Aim 3 has changed from the original application, and we provide a revised Aim 3 in this final report.

Mice lacking one or both alleles of the p53 gene develop thymic lymphomas and sarcomas[8,9]. We performed genetic screens using microsatellite analysis and BAC CGH microarrays to dissect p53-dependent or p53-independent pathways involved in radiation-induced lymphomagenesis. With this approach, we have identified the Aurora-A kinase gene within a p53-dependent amplicon on distal mouse chromosome 2. Aurora-A, a serine/threonine kinase, has been implicated in the control of chromosome segregation during mitosis and is frequently amplified in many human cancers[10-12]. Elevated expression of Aurora-A was also reported to correlate with genomic instability and clinically aggressive disease[13,14]. Interestingly, the Aurora-A gene is amplified in a substantial proportion of radiation-induced lymphomas from $p53^{+/-}$ mice (55%), but tumors from $p53^{-/-}$ mice exhibited deletions of Aurora-A in 35% of cases[15]. Further analysis suggested that the Aurora-A protein levels are tightly controlled to be compatible with ordered progression of mitosis[15]. Rapidly growing tumors from p53 null mice with high Aurora-A levels have to reduce protein levels to a tolerable range via gene deletion or possibly other unidentified mechanisms. This suggested that the oncogenic effects of Aurora-A on cancer susceptibility are dependent on the status of the p53 gene. In our other studies previously funded by DOE, we have also indentified the Aurora-A gene as a potential low

penetrance susceptibility gene based on a mouse model of skin cancer[16]. Subsequent studies showed that a single nucleotide polymorphism, T91A in the coding region of Aurora-A, that causes a Phe->Ile substitution at codon 31 is associated with susceptibility to multiple cancer types[17]. The Ile31 polymorphism in this gene is present in an estimated 5% of Caucasian and 40% of Asian populations[17]. The Ile31 variant was shown to have stronger transforming properties than the more common Phe31 allele. The Ile31 variant binds poorly to the E2 Ubiquitin-conjugating enzyme UBE2N, compared to the Phe31 variant, suggesting that this polymorphism may regulate degradation or activation of Aurora-A via an ubiquitination-mediated process[16]. However, the precise biochemical mechanisms by which the different variants function are still not well characterized. Moreover, contradictory findings regarding the Ile31 allele in conferring resistance rather than susceptibility to breast or lung cancer have been reported[18,19]. Taken together, our previous work suggested that Aurora-A may have either positive or negative effects on cell growth as a function of p53 status. It is important to understand the functional differences between these two alleles of Aurora-A in the context of different p53 backgrounds. Therefore, we hypothesized that the two different variants of Aurora-A confer differential susceptibility to tumor development in a p53-dependent manner; the Ile31 allele, with stronger oncogenic properties, functions positively in the presence of p53, but negatively in the absence of p53.

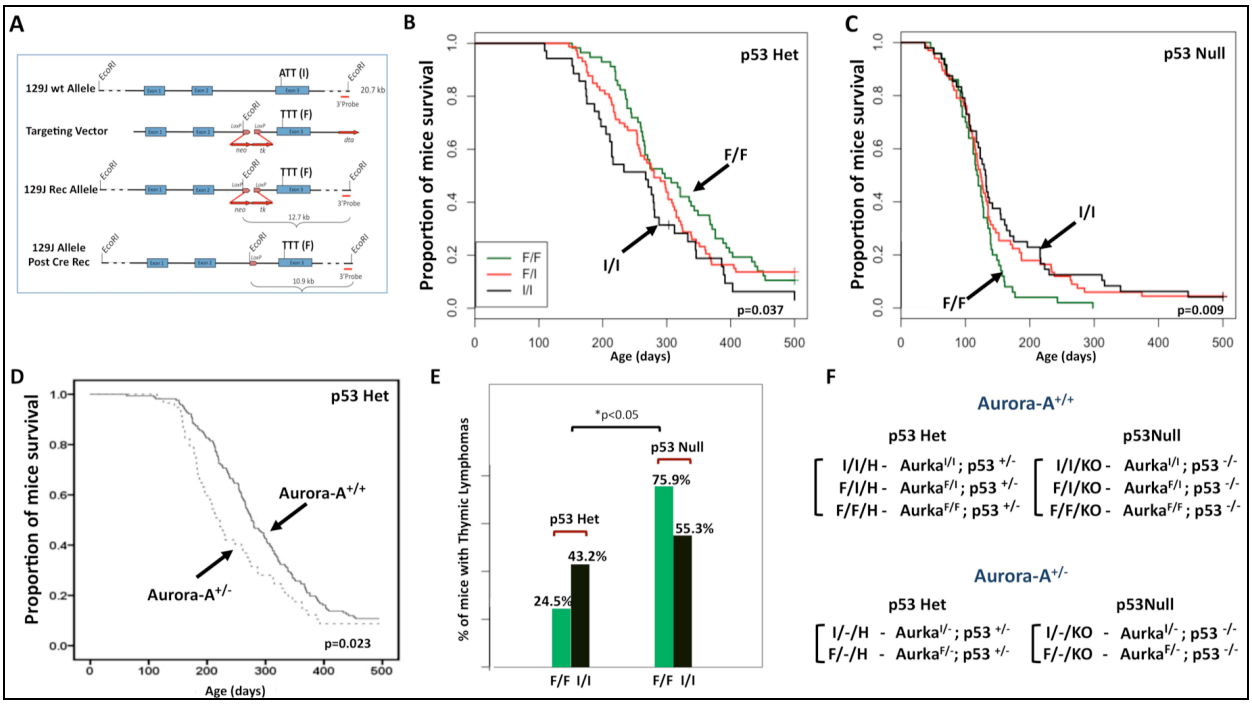

Figure 11. The effects of Phe31Ile polymorphism of the Aurora-A gene on radiation-induced lymphomagesis
A) Targeting construct for the Phe31->Ile knockin allele is shown. To create the knockin allele, a sequence change ATT->TTT was incorporated into the targeting vector. **B, C**, and **D)** Kaplan-Meier survival curves for Aurora-A knock-in/p53-deficient double mutant mice. **E)** Bar graphs illustrating % of mice that developed thymic lymphomas. **F)** A series of Aurora-A knock-in/p53-deficient double mutant mice used for the study.

To investigate the functional differences between the two alleles of Aurora-A, we have generated a knock-in mouse that carries the human-specific Aurora-A F31 allele. The knock-in strategy replaced the Ile (ATT) with Phe (TTT) at codon 31 in 129/Sv ES cells (Fig. 11A). Replacement of T91->A was verified by sequencing tail RNA of the Aurora-A heterozygous (F/I) knock-in mice (129xB6 cross). Homozygous (F/F) and heterozygous (F/I) mice for this knock-in allele were born healthy and fertile with no obvious phenotype. Growth rates of MEFs isolated

from F/F, F/I, and I/I embryos showed no significant differences (data not shown). To investigate the oncogenic properties of each variant in tumor development in the context of different p53 status, we generated a series of Aurora-A knock-in/p53-deficient double mutant mice as shown in Fig. 8F. All mice were exposed to a single dose of 4Gy whole-body γ-radiation at 5 weeks of age and observed daily until they were moribund, then sacrificed and autopsied. While the I/I genotype conferred increased risk (reduced latency) compared to the F/F genotype in the p53 heterozygous null mice (p=0.037), the reverse was observed in the p53 null mice (p=0.009, Fig. 11B and C); 43% of the I/I mice versus 25% of the F/F mice developed lymphomas in p53 heterozygous null background, while 55% of the I/I mice versus 76% of the F/F mice developed lymphomas in the p53 null background (Fig. 11E). These results support our hypothesis that the two polymorphisms confer differential susceptibility to lymphoma development in a p53-dependent manner. Interestingly, Aurora-A$^{+/-}$ heterozygous null mice (F/- and I/- on a p53 heterozygous null background) showed increased incidence and decreased latency of tumor formation compared to the Aurora-A$^{+/+}$ mice (Fig. 11D). These data suggest dual roles for Aurora-A as both an oncogene and a haploinsufficient tumor suppressor in lymphomagenesis. There exist complex regulatory mechanisms between Aurora-A and p53, emphasizing that a balanced level of Aurora-A is critical for cell survival and maintenance of genome integrity. These data highlight the critical role of interactions between common inherited genetic variants in determining tumor susceptibility, a phenomenon that may underlie the "Missing heritability" noted in GWAS in human populations.

References

1 Mao, J. H. *et al.* Fbxw7/Cdc4 is a p53-dependent, haploinsufficient tumour suppressor gene. *Nature* **432**, 775-779, doi:10.1038/nature03155 (2004).

2 Dail, M. *et al.* Mutant Ikzf1, KrasG12D, and Notch1 cooperate in T lineage leukemogenesis and modulate responses to targeted agents. *Proc Natl Acad Sci U S A* **107**, 5106-5111, doi:10.1073/pnas.1001064107 (2010).

3 Grabher, C., von Boehmer, H. & Look, A. T. Notch 1 activation in the molecular pathogenesis of T-cell acute lymphoblastic leukaemia. *Nat Rev Cancer* **6**, 347-359, doi:10.1038/nrc1880 (2006).

4 Maser, R. S. *et al.* Chromosomally unstable mouse tumours have genomic alterations similar to diverse human cancers. *Nature* **447**, 966-971, doi:10.1038/nature05886 (2007).

5 Gewinner, C. *et al.* Evidence that inositol polyphosphate 4-phosphatase type II is a tumor suppressor that inhibits PI3K signaling. *Cancer Cell* **16**, 115-125, doi:10.1016/j.ccr.2009.06.006 (2009).

6 Coustan-Smith, E. *et al.* Early T-cell precursor leukaemia: a subtype of very high-risk acute lymphoblastic leukaemia. *Lancet Oncol* **10**, 147-156, doi:10.1016/S1470-2045(08)70314-0 (2009).

7 Jen, K. Y. *et al.* Sequential mutations in Notch1, Fbxw7, and Tp53 in radiation-induced mouse thymic lymphomas. *Blood* **119**, 805-809, doi:10.1182/blood-2011-01-327619 (2012).

8 Donehower, L. A. *et al.* Mice deficient for p53 are developmentally normal but susceptible to spontaneous tumours. *Nature* **356**, 215-221, doi:10.1038/356215a0 (1992).

9 Kemp, C. J., Wheldon, T. & Balmain, A. p53-deficient mice are extremely susceptible to radiation-induced tumorigenesis. *Nat Genet* **8**, 66-69, doi:10.1038/ng0994-66 (1994).
10 Sen, S., Zhou, H. & White, R. A. A putative serine/threonine kinase encoding gene BTAK on chromosome 20q13 is amplified and overexpressed in human breast cancer cell lines. *Oncogene* **14**, 2195-2200, doi:10.1038/sj.onc.1201065 (1997).
11 Katayama, H., Brinkley, W. R. & Sen, S. The Aurora kinases: role in cell transformation and tumorigenesis. *Cancer Metastasis Rev* **22**, 451-464 (2003).
12 Meraldi, P., Honda, R. & Nigg, E. A. Aurora-A overexpression reveals tetraploidization as a major route to centrosome amplification in p53-/- cells. *Embo J* **21**, 483-492 (2002).
13 Tanaka, T. *et al.* Centrosomal kinase AIK1 is overexpressed in invasive ductal carcinoma of the breast. *Cancer Res* **59**, 2041-2044 (1999).
14 Zhou, H. *et al.* Tumour amplified kinase STK15/BTAK induces centrosome amplification, aneuploidy and transformation. *Nat Genet* **20**, 189-193, doi:10.1038/2496 (1998).
15 Mao, J. H. *et al.* Crosstalk between Aurora-A and p53: frequent deletion or downregulation of Aurora-A in tumors from p53 null mice. *Cancer Cell* **11**, 161-173, doi:10.1016/j.ccr.2006.11.025 (2007).
16 Ewart-Toland, A. *et al.* Identification of Stk6/STK15 as a candidate low-penetrance tumor-susceptibility gene in mouse and human. *Nat Genet* **34**, 403-412, doi:10.1038/ng1220 (2003).
17 Ewart-Toland, A. *et al.* Aurora-A/STK15 T+91A is a general low penetrance cancer susceptibility gene: a meta-analysis of multiple cancer types. *Carcinogenesis* **26**, 1368-1373, doi:10.1093/carcin/bgi085 (2005).
18 Sun, T. *et al.* Functional Phe31Ile polymorphism in Aurora A and risk of breast carcinoma. *Carcinogenesis* **25**, 2225-2230, doi:10.1093/carcin/bgh244 (2004).
19 Gu, J. *et al.* Polymorphisms of STK15 (Aurora-A) gene and lung cancer risk in Caucasians. *Carcinogenesis* **28**, 350-355, doi:10.1093/carcin/bgl149 (2007).